

*Letter to the Editor***3D hydrodynamical model atmospheres of metal-poor stars****Evidence for a low primordial Li abundance****Martin Asplund<sup>1</sup>, Åke Nordlund<sup>2</sup>, Regner Trampedach<sup>3</sup>, and Robert F. Stein<sup>3</sup>**<sup>1</sup> NORDITA, Blegdamsvej 17, DK-2100 Copenhagen Ø, Denmark<sup>2</sup> Astronomical Observatory, NBIfAFG, Juliane Maries Vej 30, DK-2100 Copenhagen Ø, Denmark<sup>3</sup> Department of Physics and Astronomy, Michigan State University, East Lansing, MI 48823, USA

Received: 19 April 1999 / Accepted 6 May 1999

**Abstract.** Realistic 3-dimensional (3D), radiative hydrodynamical surface convection simulations of the metal-poor halo stars HD 140283 and HD 84937 have been performed. Due to the dominance of adiabatic cooling over radiative heating very low atmospheric temperatures are encountered. The lack of spectral lines in these metal-poor stars thus causes much steeper temperature gradients than in classical 1D hydrostatic model atmospheres where the temperature of the optically thin layers is determined by radiative equilibrium. The modified atmospheric structures cause changes in the emergent stellar spectra. In particular, the primordial Li abundances may have been overestimated by 0.2–0.35 dex with 1D model atmospheres. However, we caution that our result assumes local thermodynamic equilibrium (LTE), while the steep temperature gradients may be prone to e.g. over-ionization.

**Key words:** convection – stars: abundances – stars: atmospheres – stars: Population II – line: formation

**1. Introduction**

Stellar chemical compositions are of great astrophysical importance as they carry information on stellar evolution and mixing processes, galaxy formation and evolution, and Big Bang nucleosynthesis and the baryon density of the Universe. In order to decipher the observed stellar spectra in terms of abundances a proper understanding of the line formation process is required. Often-used assumptions and approximations in abundance analyses involve 1D, plane-parallel, hydrostatic and flux-constant (radiative and convective equilibrium) model atmospheres in LTE. Free parameters such as the mixing length parameters, micro- and macroturbulence enter the model constructions and the spectral syntheses, and cause uncertainties in the derived abundances.

---

*Send offprint requests to:* martin@nordita.dk

An improved theoretical foundation for the interpretation of stellar spectra is desirable, to complement the impressive recent observational advances in terms of signal-to-noise, spectral resolution and limiting magnitudes. Modern supercomputers now allow self-consistent 3D, radiation-hydrodynamics simulations of the surface convection of late-type stars. These simulations invoke no free parameters, yet succeed in reproducing key diagnostics such as granulation topology and statistics, helioseismic properties, and spectral line shapes, shifts and asymmetries for the best available test-bench: the Sun (Stein & Nordlund 1998; Rosenthal et al. 1999; Asplund et al. 1999b). Since convection may be expected to have a prominent influence on the atmospheres of metal-poor halo stars we have performed 3D simulations for a number of such stars. In the present *Letter*, we briefly present results for two of the stars and compare emergent spectra from the 3D models with those of conventional 1D models. A full account of these and other metal-poor convection simulations will be presented elsewhere.

**2. Hydrodynamical surface convection simulations**

Realistic 3D, time-dependent, surface convection simulations of the metal-poor halo stars HD 140283 and HD 84937 have been performed using a compressible radiative-hydrodynamical code, that has previously been successfully applied to studies of the solar granulation (Stein & Nordlund 1998). The equations of mass, momentum and energy conservation coupled to the 3D equation of radiative transfer are solved on an Eulerian mesh with 100 x 100 x 82 zones, covering 35 x 35 x 12 Mm (HD 140283) and 21 x 21 x 8 Mm (HD 84937), respectively.

In order to accurately describe the photospheric layers, special care must be taken to include appropriate input physics. A state-of-the-art equation-of-state (Mihalas et al. 1988), which includes the effects of ionization, excitation and dissociation, has been used together with detailed continuous (Gustafsson et al. 1975 and subsequent updates) and line (Kurucz 1993) opacities. The 3D radiative transfer is solved for one vertical and four inclined rays under the approximations of local thermodynam-

**Table 1.** Adopted stellar parameters

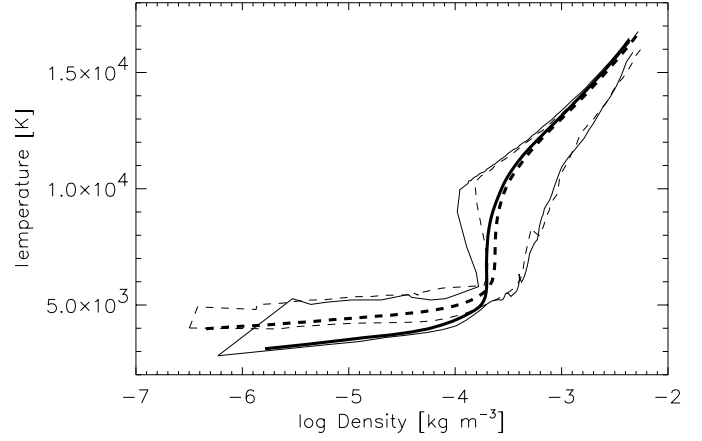
Star	$T_{\text{eff}}$ [K]	$\log g$ [ $\text{m s}^{-2}$ ]	[Fe/H]	$\xi_{\text{turb}}^a$ [ $\text{km s}^{-1}$ ]
HD 140283	5690	1.67	-2.50	1.0
HD 84937	6330	2.04	-2.25	1.0

<sup>a</sup> Not necessary for the 3D spectral line synthesis

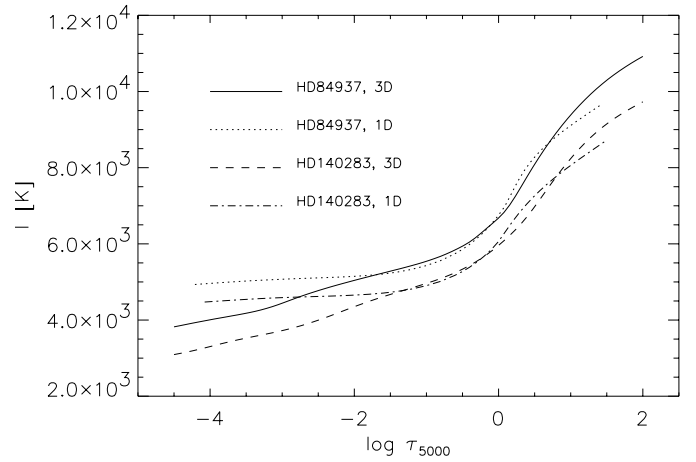
ical equilibrium (LTE) and grouping of the opacities into four bins (Nordlund 1982). The accuracy of the opacity binning procedure is verified throughout the simulations by solving the full monochromatic radiative transfer (2748 wavelength points) in the 1.5D approximation and found to always agree within 1% in emergent flux. It is noteworthy that the convection simulations contain no adjustable parameters besides those specifying the effective temperature  $T_{\text{eff}}$  (or, as used here, the entropy of the inflowing gas at the lower boundary), the gravitational acceleration at the surface  $\log g$  and the chemical composition [Fe/H]. The adopted stellar parameters, which have been obtained from the infrared flux method (IRFM, Alonso et al. 1996) for  $T_{\text{eff}}$ , Hipparcos parallaxes for  $\log g$  and published values for [Fe/H], are listed in Table 1. The individual elemental abundances are taken from Grevesse & Sauval (1998) scaled appropriately. Further details on the analogous solar simulations may be found in Stein & Nordlund (1998).

Fig. 1 shows the resulting temperature structure for the HD 140283 simulation, together with the corresponding solar simulation (Asplund et al. 1999b). The similarity between the two simulations in the deeper layers is partly fortuitous, and is due to an almost perfect cancellation of the effects of different  $\log g$  and [Fe/H]. More striking are the prominent differences in the temperature structure of the optically thin layers. While the solar simulation remains close to radiative equilibrium, much lower temperatures are encountered in the HD 140283 simulation. This seems to be a generic feature as is also present in our simulations of HD 84937 and other low-metallicity stars. The large differences also remain when comparing on optical depth scales as done in Fig. 2 where the spatial (on surfaces of equal optical depths) and temporal averages from the 3D simulations are presented together with the corresponding 1D MARCS structures.

The temperatures in the optically thin layers are predominantly determined by two competing effects: adiabatic cooling due to the expansion of ascending material and radiative heating by spectral lines (radiative heating occurs when spectral lines reabsorb some of the continuum photons whose release cause the intense cooling near continuum optical depth unity). Thus, in dynamical atmospheres the temperature tends to become depressed below its radiative equilibrium value and lines act mainly as heating agents. This is opposite to the case when radiative equilibrium is enforced in theoretical 1D model atmospheres. There, spectral lines cause surface cooling (e.g. Mihalas 1978), hence leading to shallower temperature gradients when the metallicity is diminished. In the convection simulations, the opposite happens: when decreasing [Fe/H], fewer and



**Fig. 1.** Average  $T(\rho)$  for HD 140283 (solid) compared with the Sun (dashed). Thin solid and dashed curves represent the corresponding extreme temperatures for a given density



**Fig. 2.**  $T(\tau)$  for 3D and 1D models of HD 140283 and HD 84937

weaker lines are available to absorb photons, allowing the adiabatic cooling to dominate more. As a result, balance between heating and cooling is achieved at lower surface temperatures, causing a steeper  $T(\tau)$ .

### 3. Impact on spectral line formation

Using the convection simulations as model atmospheres the 3D radiative transfer was computed under the assumption of LTE for lines of special astrophysical interest, as listed in Table 2. From the full simulations representative sequences of one hour with snapshots every 2 min were selected for the line calculations; the emergent fluxes for the shorter intervals correspond to  $T_{\text{eff}} = 5672 \pm 3$  K (HD 140283) and  $T_{\text{eff}} = 6356 \pm 8$  K (HD 84937), respectively, i.e. very close to the intended  $T_{\text{eff}}$ . Prior to the spectral synthesis the simulations were interpolated to a finer vertical resolution ( $\tau_{\text{max}} = 300$ ). The radiative transfer equation was solved for a total of 29 directions (4  $\mu$ -angles and 7 azimuthal angles plus the vertical) after which a disk-integration was carried out. Elemental abundances were derived from equivalent widths, to allow direct comparison with 1D models. It

should be noted that no micro- or macroturbulence enter the calculations, as the convective Doppler shifts and velocity gradients are sufficient to produce the observed line broadening (Asplund et al. 1999b). To estimate the impact of 3D models, a differential comparison with classical 1D MARCS model atmospheres (Gustafsson et al. 1975 with subsequent updates) was carried out, adopting a microturbulence of  $1.0 \text{ km s}^{-1}$ . The stellar parameters for the 1D models are identical to those for the shorter convection simulation sequences.

The reliability of the simulations may be assessed from a comparison between observed and predicted line asymmetries. For HD 140283 the theoretical bisectors agree very well with observations (Allende Prieto et al. 1999; Asplund et al. 1999a), e.g. in explaining the greater line asymmetries in this metal-poor star compared with solar metallicity comparison stars. The good concordance provide additional confidence in the simulations.

Due to differences in their sensitivity to the temperature structure, lines are influenced differently by the differences between 3D convection simulations and 1D model atmospheres, as is evident from Table 2. Lines of neutral minority species, low excitation transitions and stronger lines are formed in higher layers and thus feel the low temperatures there, making them stronger for a given abundance. We note for example that from the resonance line of Li I a 0.2-0.35 dex lower abundance is derived from the 3D models than from the 1D models. On the other hand, high excitation transitions and lines of ionized elements tend to result in slightly larger abundances for the 3D models, as is the case for Be II, O I and Fe II. The larger effects for the HD 140283 simulation compared with HD 84937 may be attributed to the generally stronger lines in the former due to its lower  $T_{\text{eff}}$ . Finally, we stress that the main lesson to draw from Table 2 is not the *absolute* 3D abundances but the *relative* abundances compared with differential 1D model atmospheres.

#### 4. Discussion

It is noteworthy that ionization balance of Fe is not fulfilled for the two 3D simulations, in contrast to the 1D MARCS models, which suggests that either 1) the adopted stellar parameters are inappropriate, 2) the atmospheric temperatures have been underestimated, or 3) there are significant departures from LTE present in the form of a general over-ionization of Fe of 0.3-0.6 dex. The latter effect is certainly not inconceivable, given the steep  $T(\tau)$  and the weak UV-blocking in these metal-poor environments; a 3D non-LTE investigation is clearly of high priority. One may speculate that if indeed Fe is over-ionized compared with LTE expectations, Li may also show a similar effect, in spite of the generally small non-LTE corrections in the 1D case (Carlsson et al. 1994). The possibility of erroneous  $T_{\text{eff}}$ s can most likely be refuted, since preliminary calculations reveal only minor differences ( $\lesssim 50 \text{ K}$ ) in IRFM estimates between our 3D simulations and the 1D MARCS models. The uncertainties in the stellar parameters ( $\Delta T_{\text{eff}} = 80 \text{ K}$ ,  $\Delta \log g = 0.15$ ) only correspond to  $\Delta[\text{Fe I}] = 0.10$  and  $\Delta[\text{Fe II}] = 0.08$  and can thus probably not be blamed for the discrepancy either.

**Table 2.** The derived LTE abundances of 3D hydrodynamical simulations compared with 1D hydrostatic model atmospheres (on the customary logarithmic scale where  $\log \epsilon_{\text{H}}=12.00$ )

Line [nm]	HD 140283		HD 84937	
	3D	1D <sup>a</sup>	3D	1D <sup>a</sup>
Li I 670.8	1.78	2.12	2.08	2.28
Be II 313.1	-0.92	-1.06	-0.85	-0.88
B I 249.8	-0.41	-0.21		
O I 777.2	7.20	7.15	7.32	7.30
K I 769.9	2.60	2.74		
Ca I 616.2	3.62	3.77	4.22	4.35
Fe I <sup>b</sup>	4.57 (0.16)	5.02 (0.17)	5.10 (0.12)	5.37 (0.11)
Fe II <sup>b</sup>	5.16 (0.10)	5.08 (0.11)	5.38 (0.02)	5.35 (0.03)
Ba II 614.2	-1.28	-1.12	-0.22	-0.05

<sup>a</sup> Adopting  $\xi_{\text{turb}} = 1.0 \text{ km s}^{-1}$

<sup>b</sup> 10 Fe I lines, 2 Fe II lines. The dispersions are in parenthesis

One may suspect that the very low surface temperatures have indeed been underestimated, causing systematic effects on the derived abundances. Support for such a suspicion comes from an observed trend between abundance and excitation potential for the Fe I lines, that is present with both metal-poor simulations but slightly less pronounced and in opposite direction with the 1D models; unfortunately the sample of lines is still somewhat limited however. As discussed above, it is physically very plausible to have sub-radiative equilibrium temperatures in these metal-poor environments, but the magnitude of the effect may have been overestimated. One possible reason could be the neglect of Doppler shifts in the radiative energy transfer employed in the convection simulations. In the optically thin layers the temperature is largely controlled by only a few strong lines that are partially saturated. Velocity gradients will enable the lines to absorb unattenuated continuum photons instead, thereby causing additional heating. Improved simulations addressing also this remaining refinement is planned. We note, however, that our solar simulations already predict essentially perfect agreement of line shapes and asymmetries with observations (Asplund et al. 1999b), as well as agreement for a range of other diagnostics.

Though the results presented here should be considered preliminary, pending further investigations of departures from LTE and the reality of the low surface temperature, it is still interesting to estimate possible effects on Big Bang nucleosynthesis and galactic chemical evolution.

Our 3D results suggest that the primordial Li abundance may have been overestimated by  $\approx 0.25$  dex when using classical 1D model atmospheres. Adopting  $\log \epsilon_{\text{Li}} = 2.20 \pm 0.03$  as the best estimate of the Li-plateau from a sample of metal-poor halo stars on the same  $T_{\text{eff}}$ -scale as used here (Bonafacio & Molaro 1997), we conclude that the primordial Li abundance may be as low as  $\log \epsilon_{\text{Li}} = 1.95 \pm 0.03$ , corresponding to  $\text{Li}/\text{H} = 8.9 \pm 0.6 \cdot 10^{-11}$ . It should be noted that the  $1\sigma$  uncertainties only represent the (1D) statistical errors (Ryan et al. 1999) and no corrections

for departures from LTE, post-Big Bang nucleosynthesis production of  ${}^{6+7}\text{Li}$  or stellar Li-depletion have been applied; the uncertainties are undoubtedly dominated by systematic errors. Additional simulations of metal-poor stars are important, in order to estimate more carefully the statistical errors, and also to check whether the extreme thinness of the Li-plateau found when using 1D models (Ryan et al. 1999) can be retained with 3D models. We note that our LTE Li estimate is only barely consistent with standard Big Bang nucleosynthesis predictions: if correct, our results imply that the baryon density in the Universe is  $\rho_B \approx 1.7 \cdot 10^{-31} \text{ g cm}^{-3}$  ( $\eta \approx 2.5 \cdot 10^{-10}$ ), which is in good agreement with  ${}^4\text{He}$  ( $Y_p = 0.238 \pm 0.002 \pm 0.005$ ) but at variance with both of the contested high and low D measurements (e.g. Olive 1999).

A discussion of the full impact of our results on galactic chemical evolution is clearly beyond the scope of the present paper. Instead, we very briefly point out some implications for the production of the light elements in the early Galaxy. Since Fe presumably suffers from over-ionization, [Fe] is best represented by  $[\text{Fe II}_{3D}]$  which is slightly higher than  $[\text{Fe I}_{1D}]$ . Therefore the slope [Be/H] vs [Fe/H] should remain essentially unchanged compared with 1D, i.e. close to unity. Though OH lines have not been investigated here, we anticipate a decrease of the derived O abundance with the 3D simulations, and thus that the [Be/H] vs [O/H]-relation should be shallower than in 1D. It would thus be more consistent with a primary origin for Be. Likewise we expect the [O/Fe] vs [Fe/H]-relation (based on OH-lines) to be flatter compared with the most recent findings (Israelian et al. 1998), but the claimed consistency between OH, O I and [O I] lines can no longer be expected, emphasizing the need for a non-LTE study of O based on these inhomogeneous atmospheres. Furthermore, since Be II and B I react in opposite ways to the low atmospheric temperatures, the B/Be ratio may previously have been overestimated. However, departures from LTE driven by over-ionization are significant already in 1D for B (Kiselman & Carlsson 1996) and it seems likely that in 3D the non-LTE effects will be aggravated, which may well be true also for other elements.

*Acknowledgements.* It is a pleasure to thank C. Allende Prieto, B. Freytag, B. Gustafsson, D. Kiselman, H.-G. Ludwig, P.E. Nissen and M. Steffen for rewarding discussions.

## References

- Allende Prieto C., Asplund M., Garcia-Lopez R.J., Gustafsson B., Lambert D.L., 1999, in: Theory and tests of convection in stellar structure, ASP conf. series 173, Gimenez A., Guinan E., Montesinos B. (eds.), in press
- Alonso A., Arribas S., Martinez-Roger C., 1996, A&AS 117, 227
- Asplund M., Allende Prieto C., Garcia-Lopez R.J., et al., 1999a, in preparation
- Asplund M., Nordlund Å., Trampedach R., Stein R.F., 1999b, in preparation
- Bonifacio P., Molaro P., 1997, MNRAS 285, 847
- Carlsson M., Rutten R.J., Bruls J.H.M.J., Shchukina N.G., 1994, A&A 288, 860
- Grevesse N., Sauval A.J., 1998, in: Solar composition and its evolution – from core to corona, Frölich C., Huber M.C.E., Solanki S.K., von Steiger R. (eds). Kluwer, Dordrecht, p. 161
- Gustafsson B., Bell R.A., Eriksson K., Nordlund Å., 1975, ApJ 42, 407
- Israelian G., Garcia-Lopez R.J., Rebolo R., 1998, ApJ 507, 805
- Kiselman D., Carlsson M., 1996, A&A 311, 680
- Kurucz R.L., 1993, CD-ROM No. 13
- Mihalas D., 1978, Stellar atmospheres, W.H. Freeman and Company, San Francisco
- Mihalas D., Däppen W., Hummer D.G. 1988, ApJ 331, 815
- Nordlund Å., 1982, A&A 107, 1
- Olive K.A., 1999, astro-ph/9901231
- Rosenthal C.S., Christensen-Dalsgaard J., Nordlund Å., Stein R.F., Trampedach R., 1999, A&A, in press
- Ryan S.G., Norris J.E., Beers T.C., 1999, astro-ph/9903059
- Stein R.F., Nordlund Å., 1998, ApJ 499, 914